

# The Effect of the Conductivity of Drift Chamber Walls on the Dynamics of a Relativistic Electron Beam with a Virtual Cathode

A. A. Badarin<sup>a,b</sup>, S. A. Kurkin<sup>a,b</sup>, A. A. Koronovskii<sup>a,b</sup>, and A. E. Hramov<sup>a,b\*</sup>

<sup>a</sup> Saratov State University, Saratov, 410012 Russia

<sup>b</sup> Yuri Gagarin State Technical University of Saratov, Saratov, 410054 Russia

\*e-mail: hramovae@gmail.com

Received February 10, 2015

**Abstract**—The effect of conductivity of walls of a drift chamber of the axial vircator on the behavior of a relativistic electron beam with a supercritical current was investigated. The dynamics of a relativistic electron beam is shown to be characterized by the formation of a virtual cathode of complex structure with two or three potential minima in the azimuthal direction, which rotate around the drift space axis. It is established that variation in the conductivity of drift chamber walls leads to stepwise switching of the generation frequency and a sharp change in the output power. Dependences of the output radiation power of the investigated vircator system on the conductivity of drift chamber walls for two characteristic regimes of the dynamics of a relativistic electron beam were obtained.

DOI: 10.1134/S1063785015120020

Extension of plasma-beam generators to the millimeter and submillimeter wavelength ranges and enhancement of the output radiation power of these devices are urgent problems of modern high-power microwave electronics [1–3]. One promising strategy for accomplishing this task is the development of new modifications of plasma-beam generators based on new effects established by studying the nonlinear dynamics of high-intensity relativistic electron beams (REBs) with the supercritical current in the vircator drift space [4–11]. In most theoretical studies, the walls of the electrodynamic vircator system were assumed to be ideally conducting, whereas the materials used in real experiments have finite conductivity. Therefore, one of the important problems in studying relativistic devices with a virtual cathode (VC) is investigation of the effect of loss in the electrodynamic system on the REB dynamics and output characteristics of the vircator generation.

This Letter presents results of numerical simulation of the effect of the conductivity of drift chamber walls on the dynamics of the REB with a VC using a CST Particle Studio licensed package for 3D fully electromagnetic simulation.

The system used in the investigation was a model studied previously under the assumption of ideally conducting walls [4, 6, 12]. The model is a cylindrical drift space with length  $l = 45$  mm and radius  $r = 10$  mm surrounded by a material with conductivity  $\sigma$  (drift chamber). On one end of the drift chamber, there is

a ring charged particle source (ring cathode) with inner and outer radii of 3.5 and 5 mm, respectively, which injects a tubular single-velocity electron beam; on the other end, there is a coaxial-line power output simulated by a waveguide port. The current pulse has the form of a smooth step function characterized by time  $\tau$  of rise to constant value  $I_0 = 28$  kA and total duration  $T$ . An external longitudinal homogeneous focusing field with the induction  $B_0 = 1.2$  T is applied to the system [4].

In the investigations, the current strength and external magnetic field were fixed (see above) and chosen such as to current oscillation in the VC region had the maximum amplitude in the case of ideally conducting walls, i.e., at  $\sigma \rightarrow \infty$  [4]. Here, we investigate the system dynamics upon minor variations in the control parameters, including conductivity  $\sigma$  and pulse rise time  $\tau$ . It was demonstrated that the oscillating VC is observed in a wide range of the conductivity of drift chamber walls.

During the experiments, varying conductivity  $\sigma$  of drift chamber walls, we found that the REB dynamics has two typical regimes, each being characterized by the formation of a VC with complex structure in the azimuthal direction. The first regime is characterized by the formation of two potential minima in the beam azimuthal direction, which rotate together with the electron beam around the drift space axis and form a two-turn vortex in the transit space. Such an REB

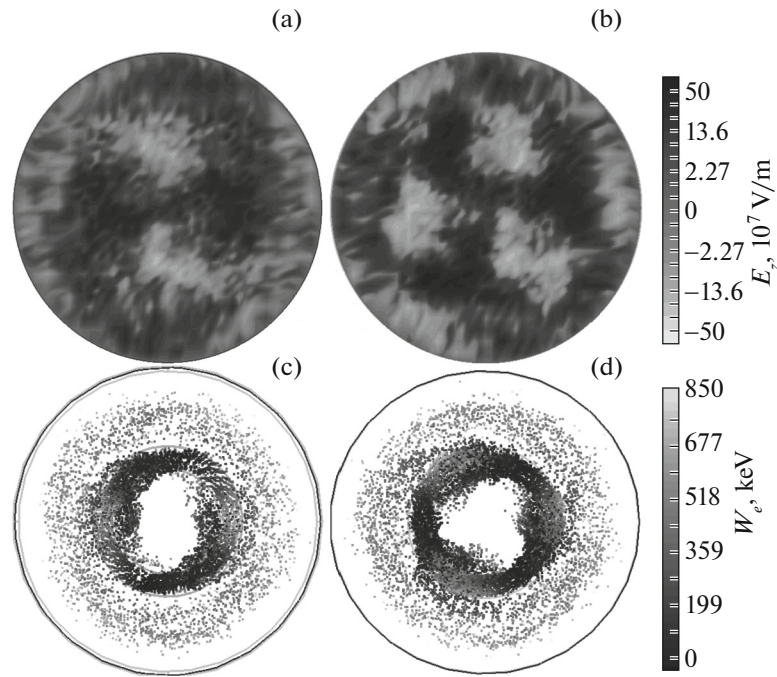


**Fig. 1.** (a, b) Instantaneous distributions of the electric field longitudinal component in the virtual cathode region and (c, d) corresponding configuration portraits of the electron beam for (a, c) regime II at  $\sigma = 10^6$  S/m and  $\tau = 3$  ns and (b, d) regime III at  $\sigma = 10^6$  S/m and  $\tau = 20$  ns. Arrows indicate electron bunches corresponding to the potential minima in the azimuthal direction.

dynamics corresponds to the formation of a VC with complex structure consisting of two electron reflection regions in the azimuth direction. Hereinafter, such behavior is called “regime II” in accordance with the number of potential minima and reflection regions of the VC. The second regime is characterized by the formation of three potential minima (regime III) and, as a consequence, a three-turn vortex and three reflection regions in the VC. Figure 1 shows the electric field longitudinal component distributions in the VC region and corresponding REB configuration portraits at different control parameters of the system corresponding to the characteristic regimes of the REB dynamics. Arrows indicate electron bunches formed in the potential minima regions (VC reflection regions) in the azimuthal direction. The figure illustrates well the qualitative difference between regimes II and III, i.e., the presence of two or three potential minima and electron bunches in the azimuthal direction, which correspond to the VC reflection regions.

The formation of vortex structures in the REB is related to the development of instabilities caused by inhomogeneity of the electron velocity field in the azimuthal and radial directions [13]. In the investigated tubular beam, the formation of vortex structures is caused by the diocotron instability [13, 14]. The configuration of the forming structures, including the number of electron bunches in the azimuthal direction, is determined by the initial perturbation of the electron beam velocity field, which leads to the devel-

opment of either azimuthal regime in the REB. In the investigated system, the beam velocity field perturbation is determined by both the interaction of particles across the common space charge field and the excitation of different modes in the used superdimensional electrodynamic system.

Along with the conductivity, an important control parameter is current pulse rise time  $\tau$ , since the current rise process strongly affects the development of instabilities, which lead to implementation of either regime. In the investigations, time  $\tau$  was varied from 1 to 25 ns. Regime II is implemented for most of the investigated conductivity values, including the case of ideally conducting walls, i.e.,  $\sigma \rightarrow \infty$ . At the same time, at pulse rise time  $\tau \sim 20$  ns and the drift chamber wall conductivity  $\sigma = 10^{4.75} - 10^{10}$  S/m, it is possible to implement the regime with three potential minima in the azimuthal direction, i.e., regime III.

It should be noted that the observed coexisting regimes are characterized by different output signal powers. Let us consider the dependences of the output electromagnetic radiation power on the conductivity of drift chamber walls for the two characteristic regimes of the dynamics, which are shown in Fig. 2 in the logarithmic scale. The solid line obtained at  $\tau = 3$  ns corresponds to regime II, and the dashed line obtained at  $\tau = 20$  ns corresponds to regime III. It can be seen that, in regime II, the power rapidly increases with an increase in the conductivity to  $\sigma_1 \approx 10^{4.75}$  S/m

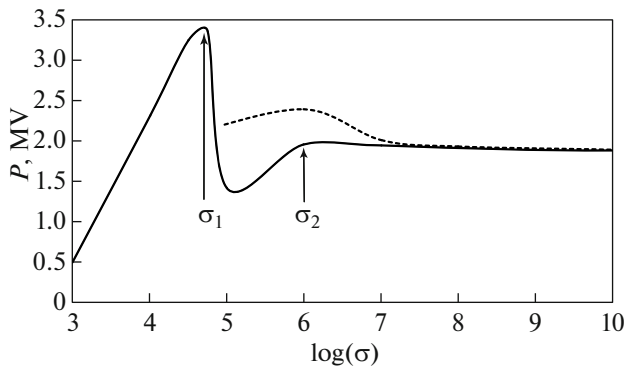


**Fig. 2.** Dependences of the output electromagnetic radiation power on the conductivity of drift chamber walls for two characteristic regimes of the dynamics in the logarithmic scale. Solid line corresponds to regime II and dashed line, to regime III.

and attains the absolute maximum; then, the output power sharply drops and rises again to  $\sigma_2 \approx 10^6$  S/m. The further conductivity growth does not lead to the noticeable variation in the output power.

Let us consider the characteristic Fourier spectra of the output signal for regime II (Figs. 3a, 3b) and regime III (Fig. 3c). It can be seen that, at the point with conductivity  $\sigma_1$ , the spectrum qualitatively changes—specifically, the fundamental harmonic frequency of the VC oscillations switches from  $f_1 \approx 43.6$  GHz to  $f_2 \approx 42.9$  GHz. In addition, in regime II the second harmonic is maximum in the spectrum until conductivity  $\sigma_1$  and the first harmonic is maximum after conductivity  $\sigma_1$  (Figs. 3a, 3b). This indicates the qualitative change in the VC dynamics.

At the initial stage of the development of generation in the investigated vircator system, the electron beam with the VC excites a wide spectrum of eigenmodes of the electrodynamic system. The mode that will be implemented should satisfy the two following conditions: (i) the electric field distributions for the mode are most similar to the beam eigenmodes and (ii) the mode frequency is most similar to the eigenfrequency of the VC oscillations, which is proportional to the REB plasma frequency [4]. Since the vircator drift chamber at the specified geometrical parameters is a superdimensional cavity with respect to the beam plasma frequency  $\omega_p \sim 30$  GHz, during the development of instability and generation in the system, the interaction with the higher-order mode occurs, which is characterized, in particular, by several field variations in the azimuthal direction. This explains the beam and field configurations resulting from the development of diocotron instability in regimes II and III. Recall that, at  $\sigma > \sigma_1$ , these two regimes coexist in the system and the establishment of either of them is determined by the mode that starts interacting with the REB at the stage of the diocotron instability devel-

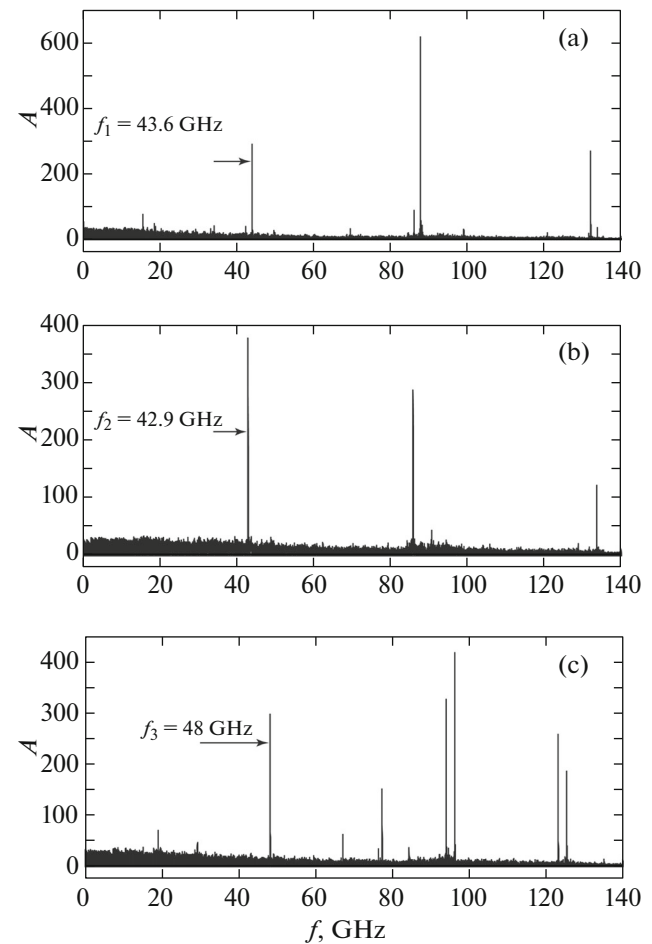


**Fig. 3.** Characteristic amplitude spectra of the output signal. (a, b) Regime II; (a) characteristic spectrum for the conductivity  $\sigma \leq \sigma_1 \approx 10^{4.75}$  S/m obtained at  $\sigma = 10^{4.75}$  S/m and  $\tau = 3$  ns, (b) characteristic spectrum for the conductivity  $\sigma > \sigma_1$  obtained at  $\sigma = 10^5$  S/m and  $\tau = 3$  ns, and (c) characteristic spectrum for regime II obtained at  $\sigma = 10^6$  S/m and  $\tau = 20$  ns.

opment, i.e., by the mode that satisfies the two above-mentioned conditions at the specified parameters and initial conditions. Thus, it turns out that the two characteristic modes with frequencies  $f_2$  or  $f_3$  corresponding to the two regimes of the dynamics of the REB with a VC satisfy these conditions. As the drift chamber conductivity is decreased, the resonance mode frequency shifts to the low-frequency region and the resonance curves corresponding to the modes diffuse due to a decrease in their Q factor. As a result of these effects, at  $\sigma \leq \sigma_1$ , the only mode with the frequency  $f_1 > f_2$  starts satisfying the two necessary conditions. This explains the frequency jump in regime II at the transition through the point with conductivity  $\sigma_1$ . The efficiency of interaction between the REB in the VC formation regime and this mode is higher; therefore, the output power increases at  $\sigma \leq \sigma_1$  (solid line in Fig. 2).

An increase in the power with conductivity in the range between  $\sigma_1$  and  $\sigma_2$  is associated with decreasing loss in space walls and the power saturation at higher conductivities is caused by the fact that, in this case, the electromagnetic wave propagating from the VC almost does not damp during its motion in the short drift space.

Let us consider the conductivity dependence of the output power for regime III with three potential minima in the azimuthal direction (dashed line in Fig. 2). It can be seen that the conductivity growth to  $\sigma_2$  leads to an increase in the output power; then, the latter decreases and tends to the curve for regime II. The output signal spectrum for regime III is presented in Fig. 3c. It can be seen that it has more high-frequency components than the spectra for regime II. The frequency of the VC fundamental harmonic  $f_3 \approx 48$  GHz is different as well. The maximum component in the spectrum is the second harmonic with frequency  $2f_3$ .

It should be noted that regime III with three potential minima in the azimuthal direction is implemented in the conductivity regions corresponding to the materials widely used in microwave devices (e.g., copper and aluminum). In addition, this regime is more promising for enhancing the vircator generation frequency due to operation at higher harmonics, since the second harmonic is maximum in the corresponding output spectrum [4].

Thus, using the numerical simulation, we established two typical regimes of the REB dynamics. Both are characterized by the formation of a VC with complex structure containing two or three potential minima in the azimuthal direction, which rotate together with the electron beam around the drift space axis and form vortex structures in the drift chamber (for more details, see [6, 12]). In addition, these regimes have different output signal spectra and different dependences of the output power on the conductivity of drift chamber walls. It was demonstrated that the regime with three potential minima in the azimuthal direction is more promising for generation at higher harmonics of the VC fundamental frequency. It should be noted that the variation in the conductivity of drift chamber walls in the regime with two potential minima in the azimuthal direction at a certain conductivity value

leads to stepwise switching of the generation frequency and a sharp change in the output power.

**Acknowledgments.** This study was supported by the Ministry of Education and Science of the Russian Federation, project order no. 3.59.2014/K and order no. 931 in the area of the providing studies. The study of the dynamics of higher harmonics of beam oscillations was supported by the Russian Science Foundation, project no. 14-12-00222.

## REFERENCES

1. D. I. Trubetskov and A. E. Khramov, *Lectures on Microwave Electronics for Physicists* (Fizmatlit, Moscow, 2004), Vol. 2 [in Russian].
2. J. H. Booske, *Phys. Plasmas* **15** (5), 055 502 (2008).
3. J. Benford, J. A. Swegle, and E. Schamiloglu, *High Power Microwaves* (Taylor & Francis, New York, London, 2007).
4. S. A. Kurkin, A. A. Badarin, A. A. Koronovskii, and A. E. Hramov, *Phys. Plasmas* **21** (9), 093 105 (2014).
5. K. R. Clements, R. D. Curry, and R. Druce, et al., *IEEE Trans. Dielec. Elec. Insulation* **20** (4), 1085 (2013).
6. S. A. Kurkin, A. E. Hramov, and A. A. Koronovskii, *Appl. Phys. Lett.* **103**, 043 507 (2013).
7. N. S. Phrolov, A. A. Koronovskii, Yu. A. Kalinin, S. A. Kurkin, and A. E. Hramov, *Phys. Lett. A* **378**, 2423 (2014).
8. A. S. Shlapakovski, T. Kwellner, Y. Hadas, Ya. E. Krasik, S. D. Polevin, and I. K. Kurkan, *IEEE Trans. Plasma Sci.* **37** (7), 1233 (2009).
9. S. A. Kurkin, A. A. Koronovskii, and A. E. Khramov, *Tech. Phys. Lett.* **37** (4), 356 (2011).
10. A. E. Dubinov and V. D. Selemir, *J. Commun. Technol. Electron.* **47** (6), 575 (2002).
11. A. N. Didenko and V. I. Rashchikov, *Sov. J. Plasma Phys.* **18**, 616 (1992).
12. A. E. Hramov, S. A. Kurkin, A. A. Koronovskii, and A. E. Filatova, *Phys. Plasmas* **19** (11), 112 (2012).
13. Yu. Ya. Golub', M. G. Nikulin, and N. E. Rozanov, *Sov. Tech. Phys.* **60** (9), 78 (1990).
14. S. I. Chung, H. J. Yun, S. B. Shim, M. Chung, and H. J. Lee, *IEEE Trans. Plasma Sci.* **39** (11), 2496 (2011).

*Translated by E. Bondareva*